Chapter 3

Mixed-Mode Delamination Failures of Quasi-Isotropic Quasi-Homogeneous Carbon/Epoxy Laminated Composite

Mahzan Johar, King Jye Wong and
Mohd Nasir Tamin

Additional information is available at the end of the chapter

http://dx.doi.org/10.5772/intechopen.69440

Abstract

This chapter characterised the delamination behaviour of a quasi-isotropic quasi-homogeneous (QIQH) multidirectional carbon/epoxy-laminated composite. The delaminated surface constituted of 45°//0 layers. Specimens were tested using mode I double cantilever beam (DCB), mode II end-notched flexure (ENF) and mixed-mode I+II mixed-mode flexure (MMF) tests at constant crosshead speed of 1 mm/min. Results showed that the fracture toughness increased with the mode II component. Specifically, the mode I, mode II and mixed-mode I+II fracture toughness were 508.17, 1676.26 and 927.52 N/m, respectively. When the fracture toughness values were fitted using the Benzeggagh-Kenane (BK) criterion, it was found that the best-fit material parameter, η, was attained at 1.21. Furthermore, fibre bridging was observed in DCB specimens, where the steady-state fracture toughness was approximately 80% higher compared to the mode I fracture toughness. Finally, through scanning electron micrographs, it was found that there was resin-rich region at the crack tip of the specimens. In addition, fibre debonding of the 45°layer was found to be dominant in the DCB specimens. Significant shear cusps were noticed in the ENF specimens. As for the MMF specimens, matrix cracking and fibre debonding of the 0°layer were observed to be the major failure mechanisms.

Keywords: mixed-mode delamination, quasi-isotropic quasi-homogeneous, laminated composite, BK criterion, scanning electron micrographs

1. Introduction

Carbon fibre reinforced polymer (CFRP) composites are widely employed in advanced structural applications such as aircraft wing skin and fuselage, automobile body panels and marine deck structures. Composites have the advantages of high specific strength and stiffness over

conventional aluminium alloy counterparts. This could greatly reduce the weight of the structure, which in turn benefits the industry through cost saving. For example, it was reported that the weight reduction of 1 kg in an aircraft structure can save over 2900 l of fuel per year [1, 2]. However, delamination is generally recognised as one of the earliest failure modes in laminated composites. This is caused by relatively low interlaminar strengths [3]. Delamination could be induced by manufacturing defects or low velocity impacts [3, 4]. This kind of damage is not easily detected [3]. Hence, the separation of the two neighbouring layers has been described as the most feared failure mechanism in laminated composites [5]. Therefore, it is essential to understand the delamination behaviour in laminated composites.

In addition, in the use of laminated composites, multidirectional laminates have been generally known to have higher interlaminar fracture toughness compared to the unidirectional laminates [6, 7]. This could be attributed to relatively blunt crack tip or intralaminar crack [7]. To study the delamination behaviour of multidirectional laminates, characterisation was commonly conducted on pure mode I, pure mode II and mixed-mode I+II tests [4, 8, 9]. It has been mentioned that the mode III component in aircraft structures could be negligible [8]. Therefore, the above-mentioned three delamination modes are the fundamental and essential loading modes to be considered.

In this chapter, the delamination behaviour of a quasi-isotropic quasi-homogeneous (QIQH) laminated composite with fibre orientation of 45° and 0° adjacent to the pre-crack was investigated. Mode I, mode II and mixed-mode I+II delamination behaviour were characterised by double cantilever beam (DCB), end-notched flexure (ENF) and mixed-mode flexure (MMF) tests. Subsequently, the variation of fracture toughness with respect to the mixed-mode ratio was fitted using the Benzeggagh-Kenane (BK) criterion. It was followed by the characterisation of R-curve behaviour of the composite. Finally, fractographic analyses were carried out on the delaminated surfaces.

2. Materials

The composite material used in this study was T600S/R368-1 carbon/epoxy prepreg supplied by Structil. The density of the prepreg was 170 g/m^2, the glass transition temperature of the resin was 105°C, the fibre volume fraction was 59 ± 2% and the average ply thickness was 0.2 mm. A 48-ply unidirectional composite laminate was fabricated using a hand lay-up technique with the stacking sequence of [0/45/90/-45/90/-45/45/-45/0/90/0/45/0/45/-45/45/90/0/90/-45/90/45/0/45//0/45/90/-45/90/-45/45/-45/0/90/0/45/0/45/-45/45/90/0/90/-45/90/-45/0/45]. The symbol '//' refers to the mid-plane location where a 15-μm Teflon film was placed to initiate the pre-crack. This provided the fibre orientation of 45°//0°adjacent to the delaminated surface. This stacking sequence led to uncoupled quasi-isotropic quasi-homogeneous (QIQH) property which was not only for the whole laminate, but also for each arm of the specimens [10]. For any 24-ply arm used here, the stiffness matrices A_{ij}, D_{ij} and B_{ij} were always the same and independent of the loading direction. Even if the laminate was not symmetric, the coupling stiffness matrix **[B]** and the entries A_{16}, A_{26}, D_{16} and D_{26} in the extensional **[A]** and bending **[D]**

http://dx.doi.org/10.5772/intechopen.69440

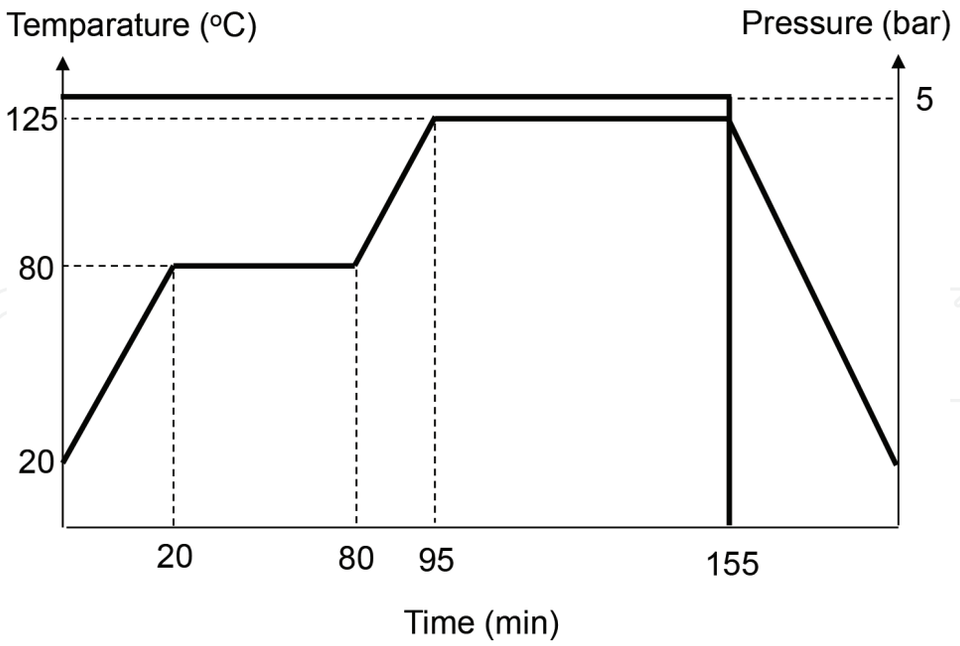

Figure 1. Curing cycle of the composite laminate fabrication.

stiffness matrices could be eliminated. Moreover, for other entries, A_{ij} was proportional to D_{ij}. This enabled random selection of fibre orientation in the layers adjacent and sub-adjacent to the interface crack. Besides, the non-dimensional ratio $D_{12}^2/(D_{11}D_{22})$ was always equal to 0.1036.

The composite was cured by using a hot-press machine according to the temperature cycle shown in **Figure 1**. Upon the completion of fabrication, the laminate was left to cool down under ambient condition.

3. Delamination tests

The composite plate was cut into specimens of 20 mm width using diamond-coated abrasive cutting blade with coolant. Three different types of fracture tests were conducted, which were double cantilever beam (DCB), 3-point end-notched flexure (ENF) and mixed-mode flexure (MMF) to characterise mode I, mode II and mixed-mode I+II delamination behaviour, respectively. The test configurations are illustrated in **Figure 2**. The composite laminate has the total thickness, $2h$ = 9.6 mm. For both ENF and MMF tests, the half-span length, L, was always set to be 60 mm. The initial crack lengths, a_o, were 40 mm for DCB specimens and 25 mm for ENF and MMF specimens. The compliances of the specimens were also measured in the range of 45–70 mm for DCB specimens and 15–55 mm for ENF and MMF specimens. This was to obtain the compliance plots for the calculation of the fracture toughness. All tests were conducted using imposed crosshead speed of 1 mm/min. At least three replicates were tested for each series of specimens. All tests were conducted under ambient condition.

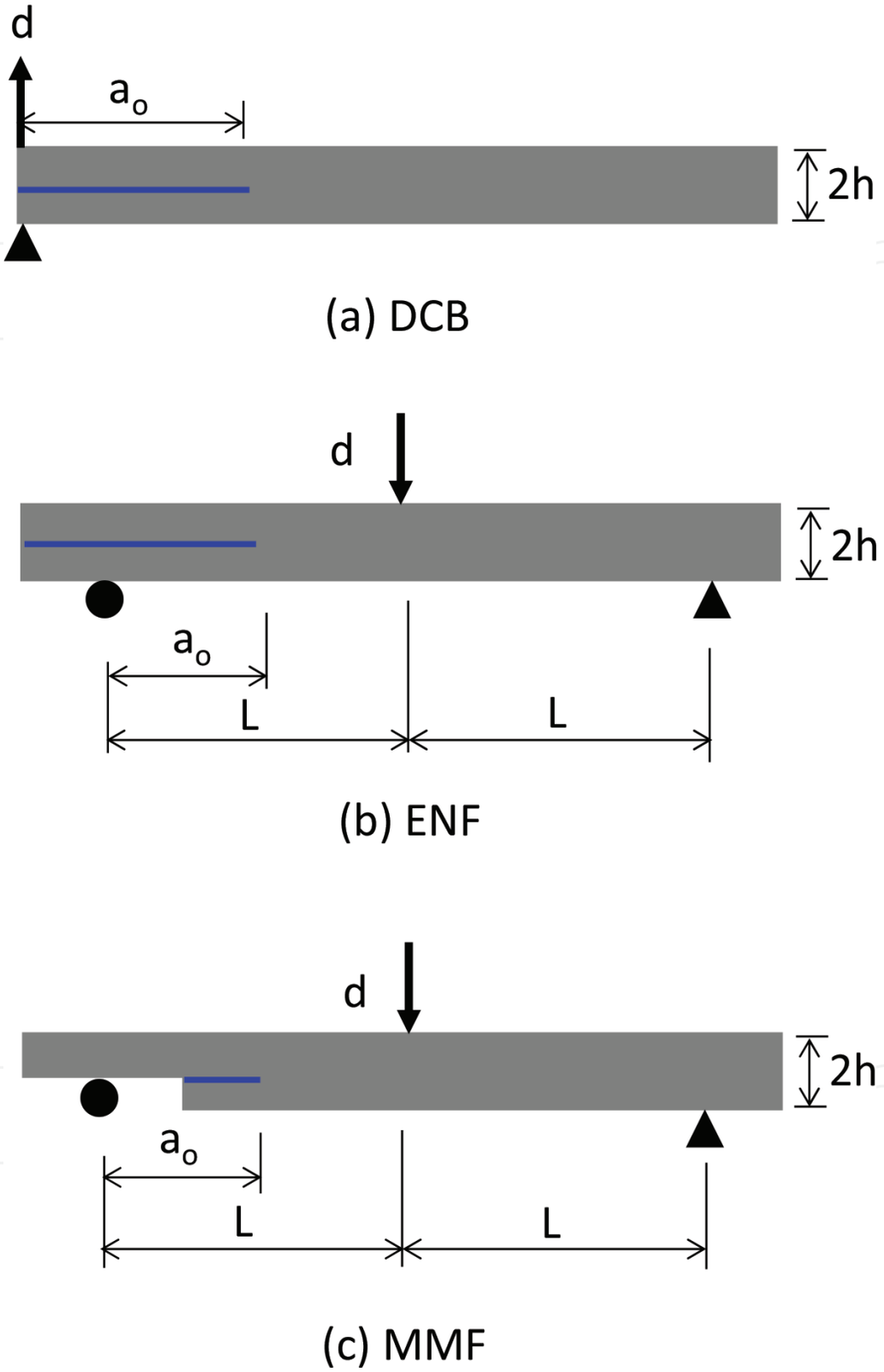

Figure 2. Test configurations for (a) DCB, (b) ENF and (c) MMF tests.

http://dx.doi.org/10.5772/intechopen.69440

4. Data reduction scheme

The analysis method for the fracture energy was based on the Irwin-Kies equation [11], which is written as

$$G_C = \left(\frac{P_C^2}{2B}\right)\left(\frac{dC}{da}\right) \tag{1}$$

where G_C is the fracture energy, P_C is the critical load attained before propagation of crack initiation, B is the width of the specimen, C is the compliance and a is the crack length. For the experimental calibration method (ECM), the empirical compliance calibrated model is expressed by

$$C = C_2 a_0^3 + C_1 \tag{2}$$

where C_2 and C_1 are obtained from C versus ${a_o}^3$ plot. Substituting the derivative of Eq. (2) into Eq. (1) yields the following expression:

$$G_C = \left(\frac{P_C^2}{2B}\right) 3C_2 a_0^2 \tag{3}$$

Eqs. (2) and (3) are also applied to the crack propagation to determine the effective crack length, a_p and the resistance to crack growth in terms of the strain energy release rate, G_p, which are described as follows:

$$a_p = \left(\frac{C_p - C_1}{C_2}\right)^{\frac{1}{3}} \tag{4}$$

$$G_p = \left(\frac{P_p^2}{2B}\right) 3C_2 a_p^2 \tag{5}$$

where C_p and P_p signify the measured specimen's compliance and the load corresponding to an effective crack length, a_p. R-curves can then be obtained in order to investigate the crack propagation behaviour.

5. Force-displacement curves

Figure 3 displays the force-displacement curves of the specimens tested using DCB, ENF and MMF tests. All tests showed initial linear region, followed by load drop after peak load (critical load) was attained. The crack propagation in the DCB specimens was comparatively less stable compared to the ENF and MMF specimens. In addition, good repeatability was observed in all tests.

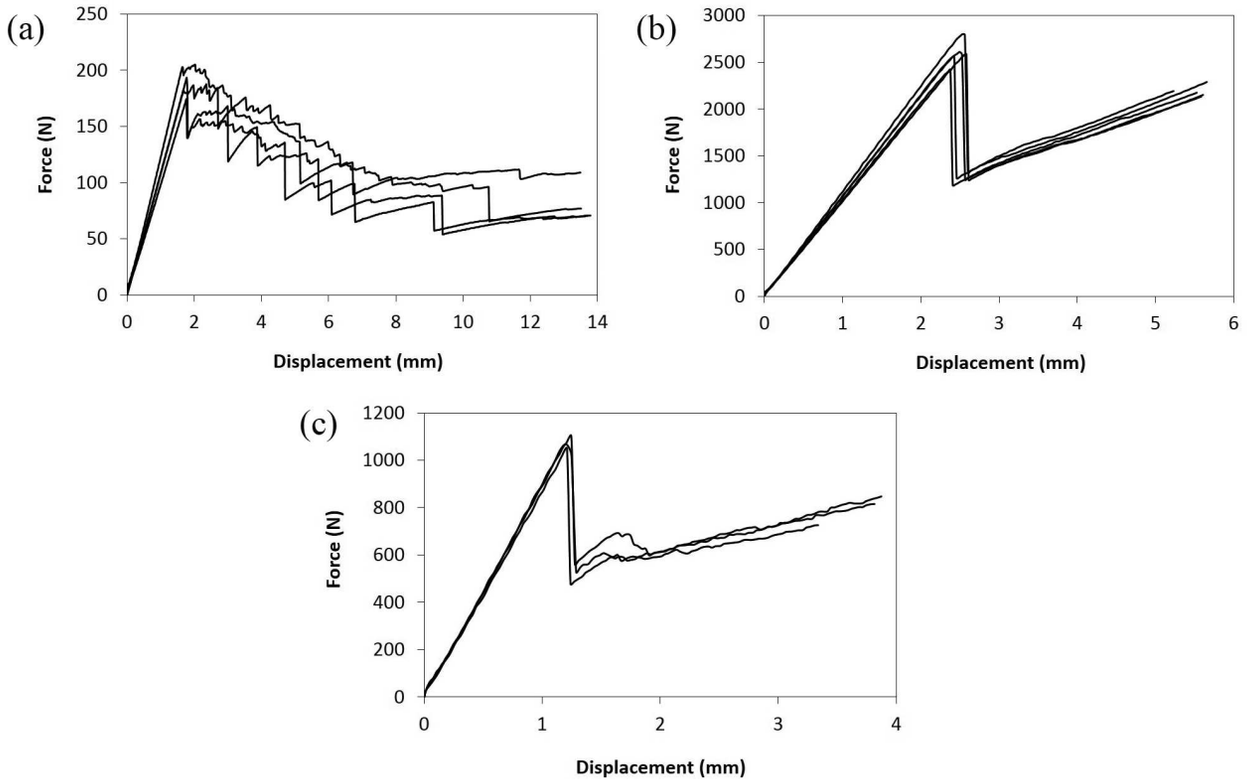

Figure 3. Force-displacement curves of (a) DCB, (b) ENF and (c) MMF specimens.

6. Mode I, mode II and mixed-mode I+II fracture toughness

The compliance plots of DCB, ENF and MMF tests are shown in **Figure 4**. By fitting the compliance data with a linear equation, C_2 and C_1 for each test were obtained and are shown in the figure. Subsequently, the fracture toughness could be calculated.

Figure 5 shows the fracture toughness at all three different mode ratios, where the values in the bracket refer to coefficient of variation (CV). The largest CV was less than 10%, which signified good repeatability of the tests. The variation of fracture toughness with respect to mixed-mode ratio was characterised using the Benzeggagh-Kenane (BK) mixed-mode criterion [12], which is expressed by Eq. (6):

$$G_{TC} = G_{IC} + (G_{IIC} - G_{IC})\left(\frac{G_{II}}{G_I + G_{II}}\right)^{\eta} \tag{6}$$

In the above equation, G_{TC} refers to the total fracture toughness for mixed-mode loading and η is the material constant and has to be determined empirically. From **Figure 5**, it could be noted that the fracture toughness increased with the mode ratio. The mode ratio, G_{II}/G_T of DCB, ENF and MMF are 0, 1 and 0.43, respectively. In addition, the best-fit η was 1.21, which was similar to the value reported for woven E-glass/bismaleimide [4], carbon/epoxy [8] and SL-EC glass-cloth/epoxy [13] composites.

http://dx.doi.org/10.5772/intechopen.69440

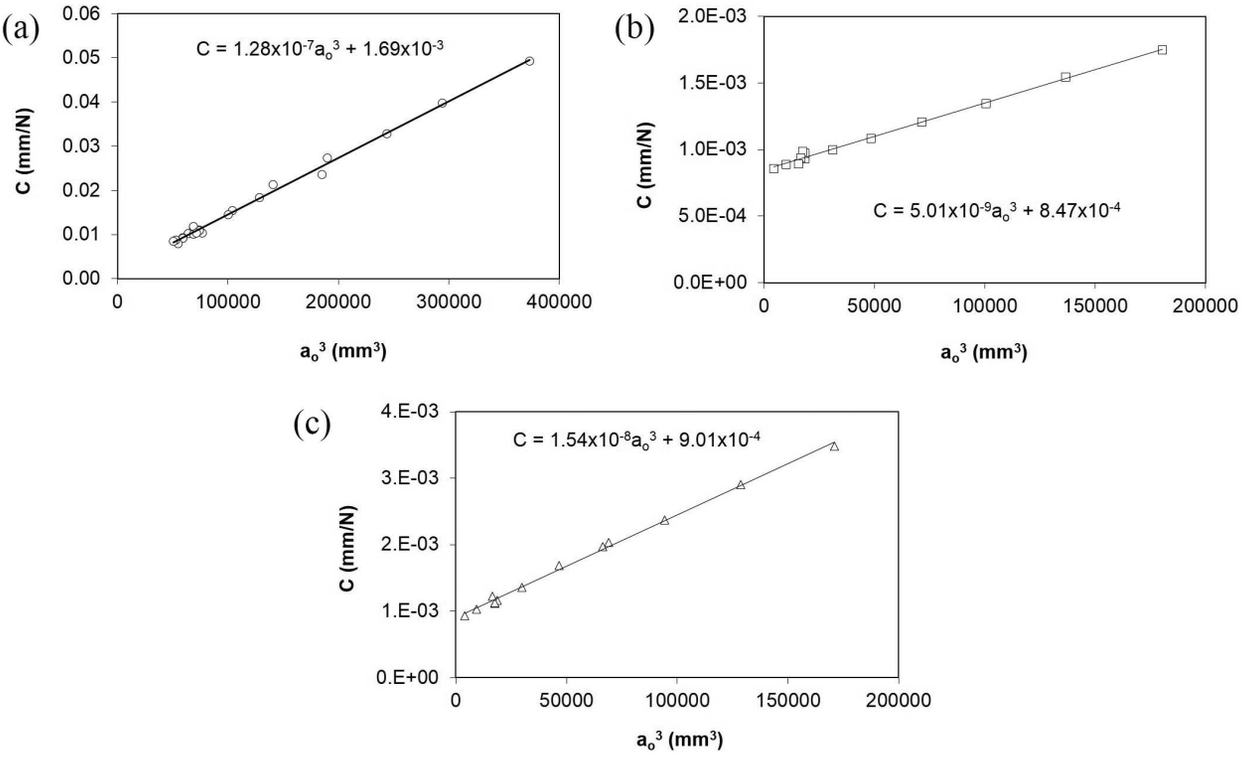

Figure 4. Compliance plots of (a) DCB, (b) ENF and (c) MMF specimens.

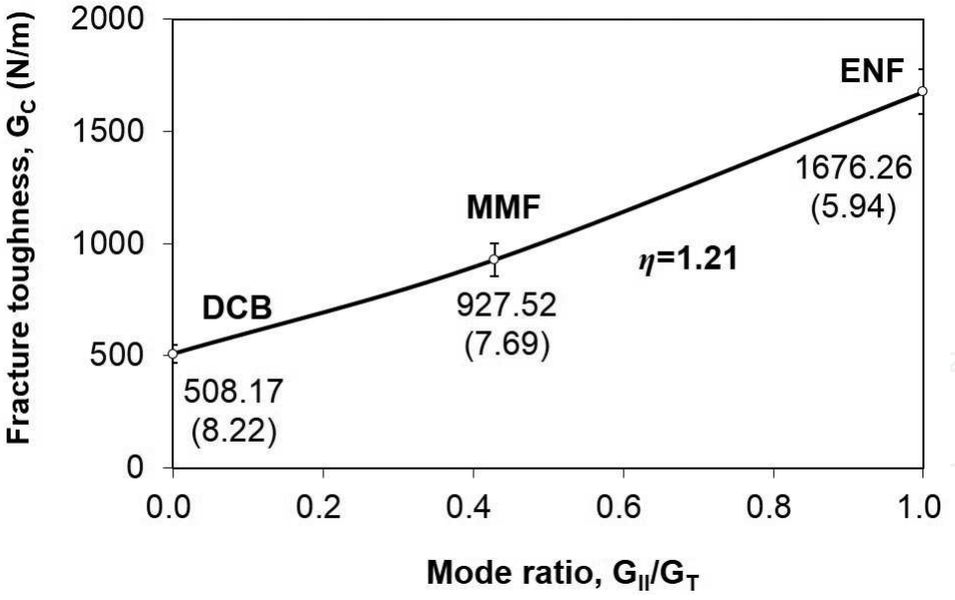

Figure 5. Variation of the fracture toughness with the mode ratio.

7. R-curve behaviour in mode I delamination

Figure 6 shows the R-curve of the DCB specimens. As shown in **Figure 6**, $da = a_p - a_o$ and $dG = G_p - G_C$, where a_p and G_p were calculated using Eqs. (4) and (5), respectively. The gaps between

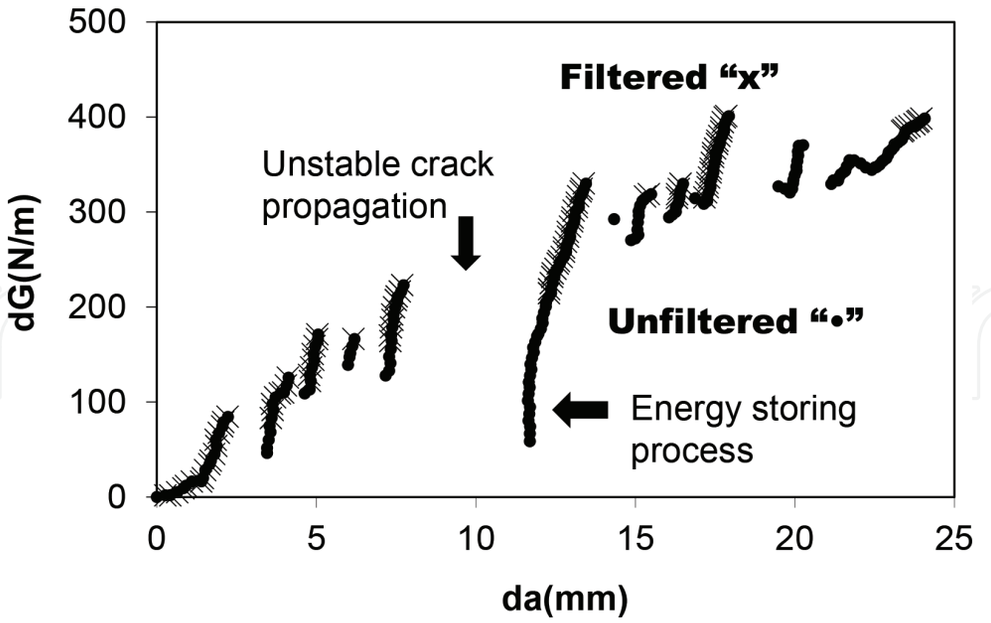

Figure 6. R-curve of the DCB specimens.

the data implied the crack jump due to instable crack propagation, where there was a sudden drop in the fracture energy. The energy magnitude of lower than the previous attained maxima did not contribute to additional crack propagation. Rather, it was an energy storing process and hence was filtered out. In this study, a drop in fracture energy of more than 5% from the previous maximum value was chosen as a basis for establishing representative R-curves. The filtered R-curve is marked as "x" in **Figure 6**. It was noted that the fracture energy increment was significant, where the maximum increment in the fracture energy (≈400 N/m) was approximately 80% of the G_{IC} value.

8. Fractographic analyses

Figures 7–9 show the comparison of the scanning electron micrographs of the delaminated surfaces of DCB, ENF and MMF specimens at the crack-tip region. It is obvious that there was significant resin-rich region at the crack tip of DCB and MMF specimens. In addition to the resin-rich region, fibre debonding was also found to be relatively significant in MMF specimen. As for the ENF specimen, matrix cracking and fibre debonding were found to be the two major damage mechanisms. This suggested that the fracture toughnesses that were calculated at different modes were actually contributed by the energy dissipation by different damage mechanisms.

To further investigate the delamination behaviour in the delamination region, additional scanning electron micrographs were captured and are shown in **Figures 10–12**. It was observed that for the DCB specimen, the delamination was dominated by the 45° layer, where fibre debonding was the major failure mechanism. Even on the 0° surface, traces of 45°layer

http://dx.doi.org/10.5772/intechopen.69440

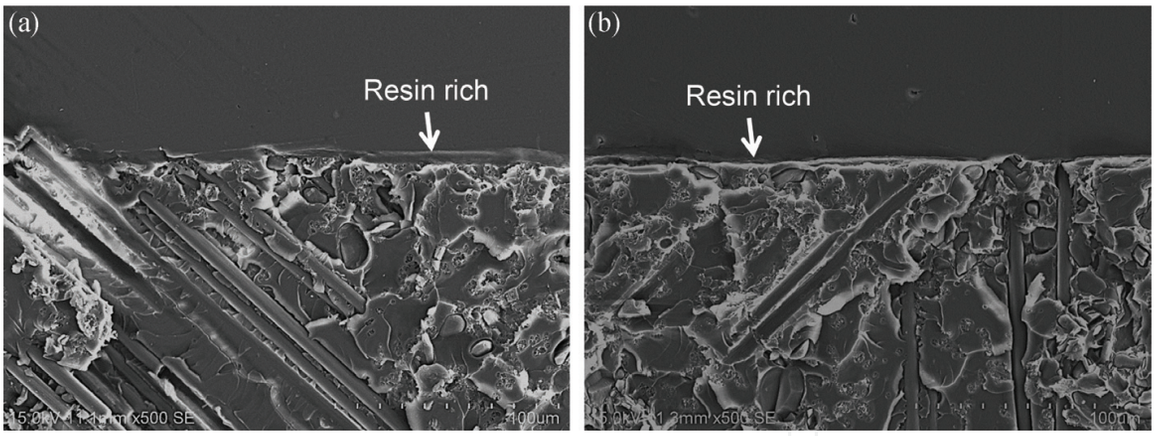

Figure 7. Crack-tip delamination of the DCB specimen: (a) 45°layer and (b) 0°layer.

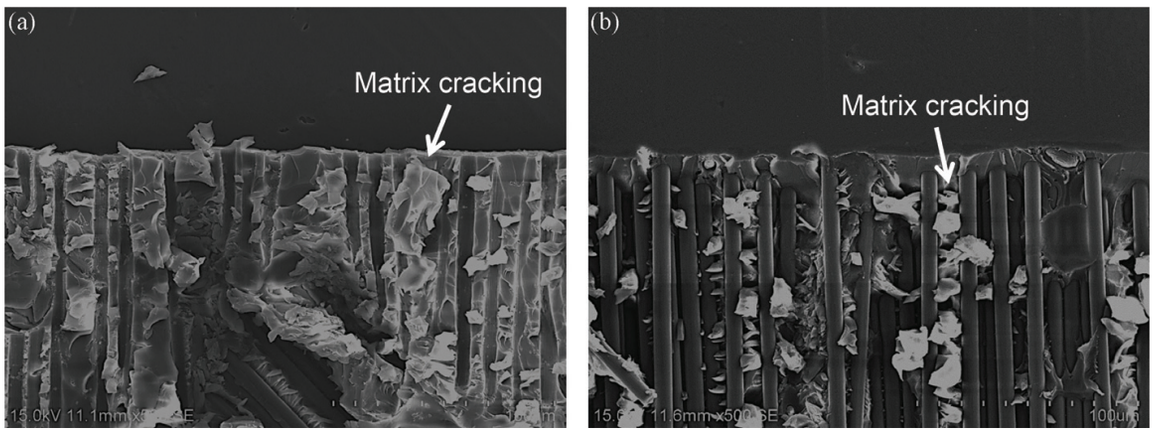

Figure 8. Crack-tip delamination of the ENF specimen: (a) 45°layer and (b) 0°layer.

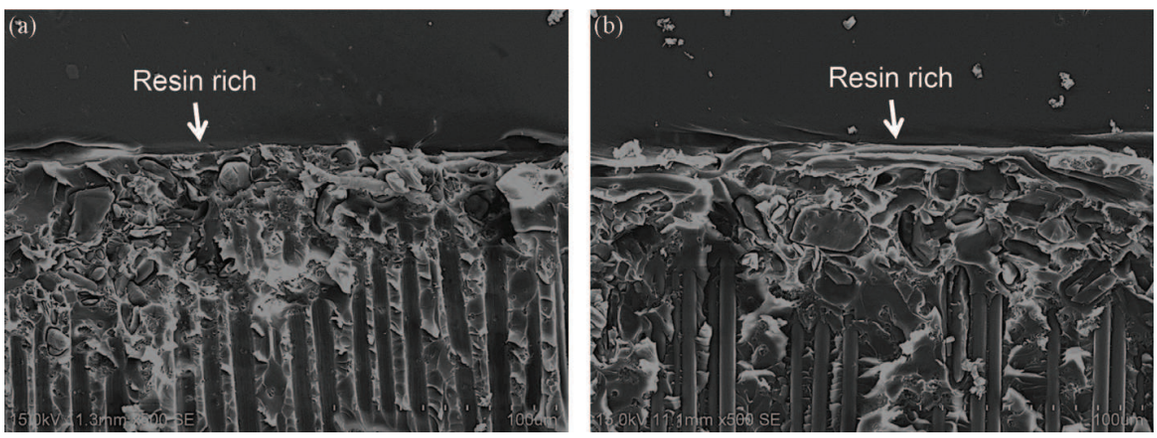

Figure 9. Crack-tip delamination of the MMF specimen: (a) 45°layer and (b) 0°layer.

were observed. Based on the R-curve behaviour observed, it was thus believed that fibre debonding has led to fibre bridging that enhanced the delamination growth and dissipated additional fracture energy [14].

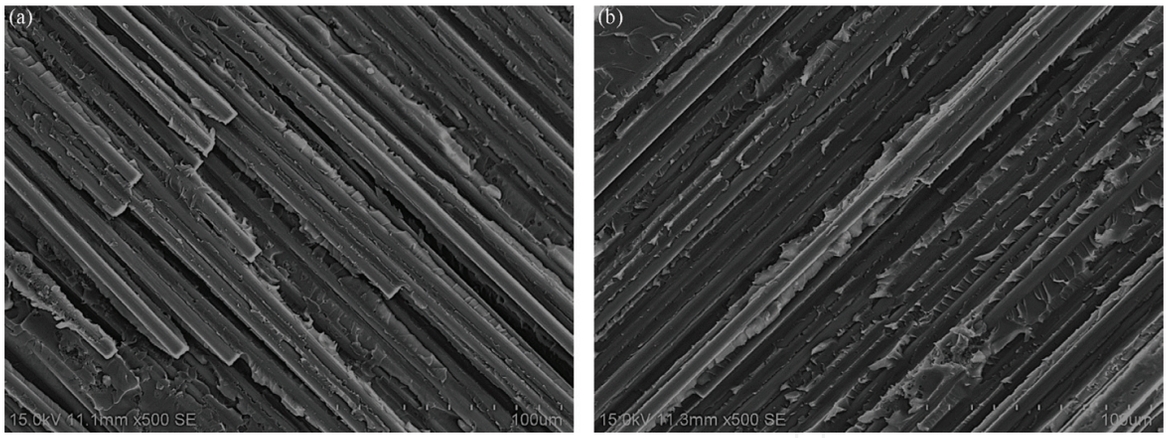

Figure 10. Delamination surfaces of the DCB specimen: (a) 45°layer and (b) 0°layer.

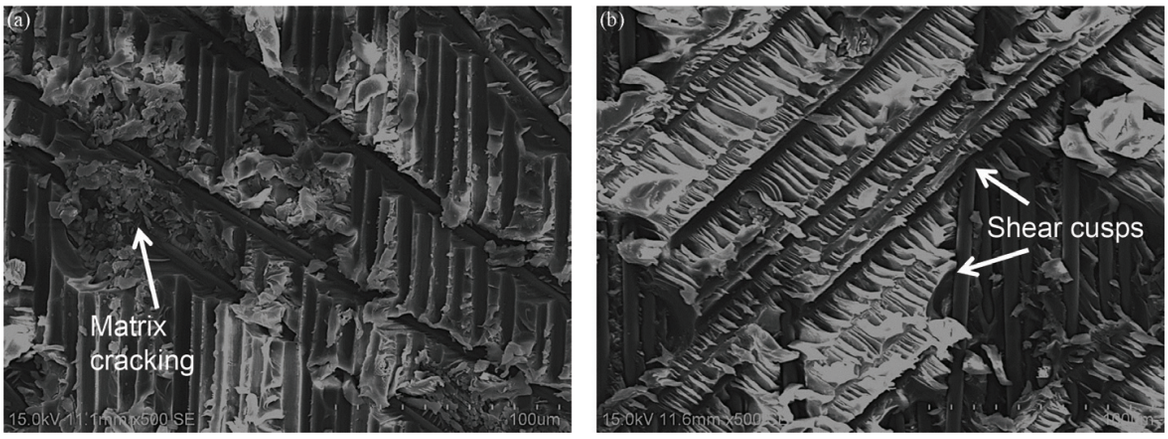

Figure 11. Delamination surfaces of the ENF specimen: (a) 45°layer and (b) 0°layer.

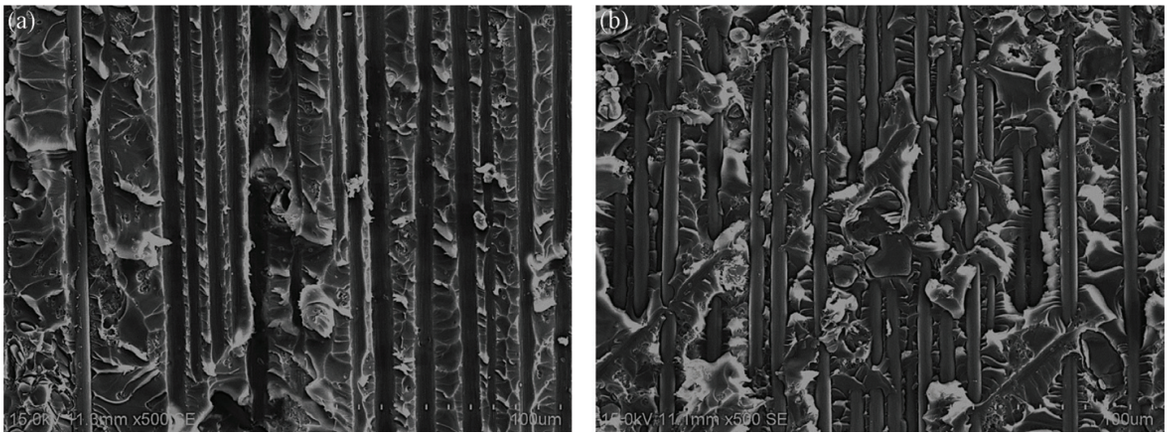

Figure 12. Delamination surfaces of the MMF specimen: (a) 45°layer and (b) 0°layer.

http://dx.doi.org/10.5772/intechopen.69440

As for the ENF specimen, a significant difference in the delamination behaviour was observed. Fibre debonding was observed on the fibres in the 0°direction. However, significant shear cusps were observed on the 0°layer in the 45° direction, which was attributed to the shear mode loading. It has also been reported that the high shear mode would draw large shear cusps [6, 7]. A certain amount of matrix cracking was observed on the 45° layer, which was believed to be due to the interaction between 0°and 45° layers during shearing. Matrix hackles were also observed in the ENF specimen of a woven E-glass/bismaleimide composite [4].

As for the mixed-mode delamination, the MMF specimen exhibited fibre debonding dominated by the 0° layer, which was similar to the ENF specimen. Nevertheless, the shear cusps in the MMF specimen were less significant and more random compared to the ENF specimen, which was similar to the observation by Naghipour et al. [6]. In addition, the roughness of the MMF specimen was less than the ENF specimen [7]. On the other hand, matrix cracking seemed to be another major failure mechanism. All these observations suggested that the modes of loading influenced the failure mechanisms of the specimens, which in turned reflected in different values of fracture toughness.

9. Conclusion

In order to evaluate the delamination behaviour of a multidirectional laminated composite with 45° and 0° layers adjacent to the pre-crack, a quasi-isotropic quasi-homogeneous (QIQH) composite laminate was fabricated. Double cantilever beam (DCB), end-notched flexure (ENF) and mixed-mode flexure (MMF) tests were carried out to characterise mode I, mode II and mixed-mode I+II delamination, respectively. All tests were conducted at a constant crosshead speed of 1 mm/min under ambient condition. The average fracture toughnesses were mode I G_{IC} = 508.17 N/m, mode II G_{IIC} = 1676.26 N/m and mixed-mode I+II $G_{(I+II)C}$ = 927.52 N/m. The best-fit material parameter, η = 1.21, according to the Benzeggagh-Kenane (BK) criterion. Through scanning electron micrographs, the crack-tip region was found to be resin-rich. In addition, fibre debonding of the 45° layer was dominant in the DCB specimen, which was believed to have led to fibre bridging behaviour. Furthermore, in the ENF specimen, significant shear cusps were observed. Finally, matrix cracking and fibre debonding of the 0° layer were observed in the MMF specimen.

Acknowledgements

This work is supported by Ministry of Higher Education Malaysia and Universiti Teknologi Malaysia through Fundamental Research Grant Scheme (FRGS) No. 4F591. The authors also acknowledge Institut Supérieur de l'Automobile et des Transports (ISAT), France for providing the facilities for fabrication and testing.

Author details

Mahzan Johar, King Jye Wong* and Mohd Nasir Tamin

*Address all correspondence to: kjwong@mail.fkm.utm.my

Faculty of Mechanical Engineering, Universiti Teknologi Malaysia, Johor Bahru, Malaysia

References

[1] Soutis C. Fibre reinforced composites in aircraft construction. Progress in Aerospace Sciences. 2005;**41**(2):143-151. DOI: 10.1016/j.paerosci.2005.02.004

[2] Soutis C. Carbon fiber reinforced plastics in aircraft construction. Materials Science and Engineering A. 2005;**412**(1-2):171-176. DOI: 10.1016/j.msea.2005.08.064

[3] Turon A, Camanho PP, Costa J, Davila CG. A damage model for the simulation of delamination in advanced composites under variable-mode loading. Mechanics of Materials. 2006;**38**(11):1072-1089. DOI: 10.1016/j.mechmat.2005.10.003

[4] Zhao Y, Liu W, Seah LK, Chai GB. Delamination growth behavior of a woven E-glass/bismaleimide composite in seawater environment. Composites Part B: Engineering. 2016; **106**:332-343. DOI: 10.1016/j.compositesb.2016.09.045

[5] Pagano NJ, Schoeppner GA. Delamination of polymer matrix composites: Problems and assessment. In: Kelly A, Zweben C, editors. Comprehensive Composite Materials. Oxford: Pergamon; 2000. pp. 433-528. DOI: 10.1016/B0-08-042993-9/00073-5

[6] Naghipour P, Schneider J, Barsch M, Hausmann J, Voggenreiter H. Fracture simulation of CFRP laminates in mixed mode bending. Engineering Fracture Mechanics. 2009;**76**(18): 2821-2833. DOI: 10.1016/j.engfracmech.2009.05.009

[7] Naghipour P, Bartsch M, Chernova L, Hausmann J, Voggenreiter H. Effect of fiber angle orientation and stacking sequence on mixed mode fracture toughness of carbon fiber reinforced plastics: Numerical and experimental investigations. Materials Science and Engineering A. 2010;**527**(3):509-517. DOI: 10.1016/j.msea.2009.07.069

[8] LeBlanc LR, LaPlante G. Experimental investigation and finite element modeling of mixed-mode delamination in a moisture-exposed carbon/epoxy composite. Composites Part A: Applied Science and Manufacturing. 2016;**81**:202-213. DOI: 10.1016/j.compositesa.2015.11.017

[9] Liu Y, Zhang C, Xiang Y. A critical plane-based fracture criterion for mixed-mode delamination in composite materials. Composites Part B: Engineering. 2015;**82**:212-220. DOI: 10.1016/j.compositesb.2015.08.017

[10] Vannucci P, Verchery G. A new method for generating fully isotropic laminates. Composite Structures. 2002;**58**(1):75-82. DOI: 10.1016/S0263-8223(02)00038-7

[11] Irwin GR, Kies JA. Critical energy rate analysis of fracture strength. Welding Journal Research Supplement. 1954;**33**:193-198

[12] Benzeggagh ML, Kenane M. Measurement of mixed-mode delamination fracture toughness of unidirectional glass/epoxy composites with mixed-mode bending apparatus. Composites Science and Technology. 1996;**56**(4):439-449. DOI: 10.1016/0266-3538(96)00005-X

[13] Shindo Y, Shinohe D, Kumagai S, Horiguchi K. Analysis and testing of mixed-mode interlaminar fracture behavior of glass-cloth/epoxy laminates at cryogenic temperatures. Journal of Engineering Materials and Technology. 2005;**127**(4):468-475. DOI: 10.1115/1.2019944

[14] Barikani M, Saidpour H, Sezen M. Mode-I interlaminar fracture toughness in unidirectional carbon-fibre/epoxy composites. Iranian Polymer Journal. 2002;**11**(6):413-423

IntechOpen